Referee #2

Overall evaluation:

The study presented in this paper investigates the individual and synergistic assimilation of satellite microwave soil moisture products from three sensors at different frequencies (SMAP at L-band, ASCAT at C-band, and MWRI at X-band) into the Common Land Model (CoLM). The skill of the various data assimilation experiments as well as the skill of forecasts initialized from the respective analyses is evaluated against soil moisture observations from the ERA5-Land reanalysis, as well as in situ soil moisture observations from the International Soil Moisture Network (ISMN) and the Chinese Meteorological Administration (CMA). The authors find that generally the combination of all three sensors yields the best performance, except over densely vegetated areas where the inclusion of X-band retrievals leads to a skill degradation. To address this, they present a vegetation-adaptive data assimilation framework that shows slightly better overall performance.

Overall, this is an interesting paper, and the inclusion of X-band observations offers a novel and valuable perspective. However, several major issues need to be addressed before the manuscript can be considered for publication.

Response:

We sincerely thank you for your valuable time and professional guidance. Your comments have greatly improved the quality of this manuscript.

In the methodology section, we have provided additional details on satellite observation preprocessing and model configuration. Specifically, we have included the quality control criteria corresponding to the original quality flags of each sensor, described the CDF-based bias correction applied to the second soil layer, and clarified the rationale for selecting this layer for assimilation. We have also added a detailed description of the 10-layer soil structure in the CoLM model, along with its spatial and temporal resolution, as well as the screening criteria for CMA and ISMN in situ observations. Regarding error estimation and the assimilation procedure, we have provided a more explicit description. In regions with in situ observations, we apply the Triple Collocation method to estimate the independent errors of each data source. In regions without station coverage, the RMSE with respect to ERA5-Land soil moisture is used as a surrogate estimate. In addition, we have clarified the quality control procedures in the assimilation system, including the exclusion of frozen soil and water grid cells, as well as the filtering of observations whose innovations exceed three standard deviations. We have also added further justification for the necessity of the vegetation-adaptive framework.

In the results section, we have standardized the naming of the experiments (DA_L, DA_C, DA_X) following the reviewer's suggestion, and supplemented the statistical figures with 95% confidence intervals, the number of validation sites, and the corresponding physical units. To further enhance the robustness of our conclusions, we conducted additional multi-season experiments. The new results further support our conclusion that, in the assimilation application of X-band products, introducing physical constraints related to vegetation type and optimizing data screening can lead to more stable additive improvements from X-band assimilation. Moreover, through the comparative analysis of multi-season assimilation performance, we found that, in addition to vegetation type, the seasonal variation of vegetation should also be considered when assessing the impact of X-band assimilation. These additional findings further strengthen the scientific value of the manuscript.

Below, we provide a detailed point-by-point response to your comments, and the corresponding revisions in the manuscript have been highlighted in a specific color.

Major Comments:

1. This paper lacks essential details regarding the methodology that are needed to properly assess and interpret the results presented. In addition, several statements within the methodology section appear contradictory, further complicating the interpretation of the findings. Specifically:

1.1 More detail is needed regarding the preprocessing of the satellite observations. For example, what form of quality control is applied for each of the satellite datasets? Is this based on quality flags provided with each product? Are the observations bias-corrected to the model climatology? The authors mention that "the retrieved soil moisture from satellite products is mapped to the model's second soil layer". Does that mean the retrievals are CDF-matched to the second layer soil moisture or is a different approach chosen? Why was the second soil layer selected and what is the depth of this layer in CoLM?

Response:

Thanks for your suggestions. Following your suggestions, we revised the description of satellite observation preprocessing in the data section (Section 2) of the revised manuscript. The revised text clarifies the procedures for quality control, bias correction, and the mapping between satellite observations and the model soil layers. The added text can be found in Lines 236–243 of the revised manuscript, as follows:

Before assimilation, quality control was conducted for each satellite dataset, primarily based on their native quality flags. For SMAP, we kept retrievals with quality flags of 0 or 8. For ASCAT, we retained observations with an aggregated quality flag below 50% (Chen et al., 2018). For FY3D, only observations with a quality flag of 0 were used.

We then performed bias correction using cumulative distribution function (CDF) matching. Specifically, satellite-derived soil moisture was matched to the CoLM background simulations for summer 2022 and then mapped to the model's second soil layer, consistent with Albergel et al. (2017). This layer was selected because it better matches the effective sensing depth of the satellite products. In this CoLM setup, the top layer is 0–1.75 cm thick and responds quickly to rainfall, evaporation, and surface thermal forcing, so it mainly captures short-lived surface fluctuations. The second layer, which spans 1.75–4.51 cm, is closer to the main sensing depth of SMAP and ASCAT (about 0–5 cm) and provides a more stable representation of near-surface soil moisture. It was therefore used for observation mapping and bias correction.

The following references are cited here and were already included in the original manuscript:

Albergel, C., Munier, S., Leroux, D. J., Dewaele, H., Fairbairn, D., Barbu, A. L., Gelati, E., Dorigo, W., Faroux, S., Meurey, C., Le Moigne, P., Decharme, B., Mahfouf, J.-F., and Calvet, J.-C.: Sequential assimilation of satellite-derived vegetation and soil moisture products using SURFEX_v8.0: LDAS-Monde assessment over the Euro-Mediterranean area, Geosci. Model Dev.,

10, 3889–3912, https://doi.org/10.5194/gmd-10-3889-2017, 2017.
Chen, F., Crow, W. T., Bindlish, R., Colliander, A., Burgin, M. S., Asanuma, J., and Aida, K.: Global-scale evaluation of SMAP, SMOS and ASCAT soil moisture products using triple collocation, Remote Sens. Environ., 214, 1–13, https://doi.org/10.1016/j.rse.2018.05.008, 2018.

1.2 More details are needed regarding the actual data assimilation. How is the observation error for each of the three satellite products defined? The authors mention that the observation error statistics are derived from the RMSE between the open loop (CTL) and ERA5, but it is unclear how this would provide any information about the uncertainty of the three satellite retrieval products. Also please specify what quality control is applied within the assimilation system. For example, do you assimilate observations over frozen soils, when there are open water bodies present in the grid cell, or if the departures between the model background and the observations are very large?

Response:

Thanks for your suggestions. In the revised manuscript, we have expanded this part in Section 3.3 (Lines 347–355) and added Figure R4 to the revised manuscript as Figure 4 to illustrate the spatial distributions of observation errors and background errors. The added text is as follows:

For areas without station observations, errors are characterized by the root-mean-square error (RMSE) against the ERA5-Land product. In station-covered regions, observation and background errors are estimated via TC using CoLM simulations, in-situ data, and satellite retrievals as independent inputs. These TC estimates were scaled to match RMSE magnitudes to ensure consistency. Spatial patterns of these errors are shown in Figure 4. Based on these estimated errors, and following de Rosnay et al. (2013), we specified both the background and observation error covariance matrices as diagonal, with their diagonal entries derived from the errors. In the assimilation process, only land pixels are considered according to CoLM's underlying surface data, while inland water and frozen soil grids are masked. Additionally, a 3-sigma innovation check is applied, rejecting any observations that deviate from the background by more than three standard deviations.

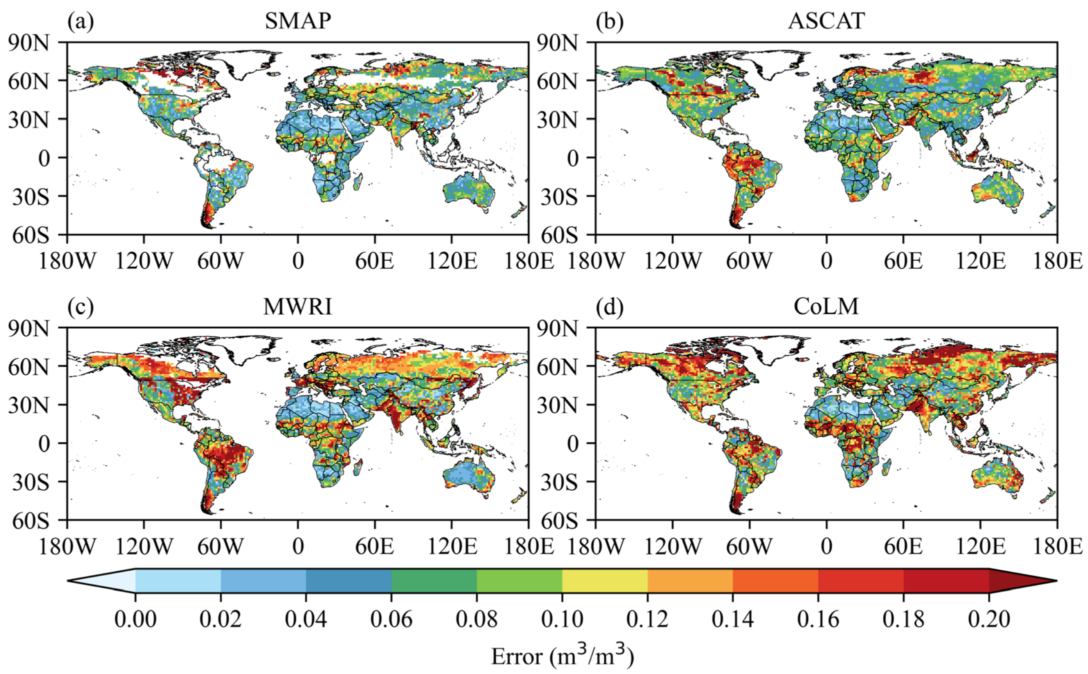

Figure R1: Spatial distributions of observation and background errors for different satellites. (a) SMAP observation error; (b) ASCAT observation error; (c) MWRI observation error; and (d) CoLM background error.

1.3 More details regarding the model are needed, specifically the distribution of the seven soil layers and the temporal resolution of the model outputs.

Response:

Thanks for your suggestions. Following your suggestions, we revised the description of the CoLM model configuration, with particular attention to the soil layer structure, spatial resolution, and temporal resolution. The key added text can be found in Lines 284–286 and Lines 294–295 of the revised manuscript, as follows:

Specifically, the bottom depths of these 10 layers are 1.75, 4.51, 9.06, 16.55, 28.91, 49.29, 82.89, 138.28, 229.61, and 380.19 cm, respectively.

For the simulations conducted in this study, the model is configured with a horizontal spatial resolution of 1.4° × 1.4° and an output temporal resolution of 1 hour.

1.4 More details are needed about the processing of the in situ station data. Was any quality control applied based on the quality flags, the observing conditions (e.g., frozen soil), or the completeness of the observation time series? How many stations were used in total? It is also unclear which in situ networks are used when. The methodology section mentions both ISMN and CMA, but the map plots in the results section (Figures 12 and 13) only show stations in China and the text for Figure 6 also mentions that only stations in China are used. Which of the figures in the results section include the ISMN data? Please label all plots clearly to show which networks were used.

Response:

Thanks for your suggestions. In the revised manuscript, we have added detailed information on the quality control procedures for station data, the number of stations used, and the observation networks corresponding to each figure. In addition, Figure R1 has been included in the revised manuscript as Figure 2 to more clearly illustrate the spatial coverage of the in-situ stations.

We would also like to clarify that there was an error in the description of Figure 6 in the original manuscript. The statement that "Figure 6 only uses stations from China" was incorrect. In fact, all overall statistical analyses in this study are based on the full set of valid stations from both the ISMN and CMA networks. This error has been corrected in the revised manuscript.

The added text (Lines 248–254) is as follows:

To ensure data reliability, quality control was performed based on the original quality flags provided by each network prior to validation, retaining only valid measurements. For the ISMN dataset, which includes the USCRN, COSMOS-UK, SOILSCAPE, ARM, TAHMO, SMOSMANIA, and FR_Aqui networks, we utilized the station-specific quality flags and only kept observations marked as 'G'. Similarly, only valid observations with a quality flag of 0 were retained for the CMA network. To maximize the spatial coverage for evaluation, this study did not impose a strict threshold on time-series completeness during the quality control process, ensuring that all valid observations passing the physical screening were included in the analysis.

A total of 3057 stations remained after these quality control procedures. Figure R2 illustrates the spatial distribution of the CMA and ISMN in-situ stations to provide a clear visualization of the ground-based data coverage. Among these, 2792 CMA stations are densely distributed across most of China as shown in Figure R2a. Additionally, a total of 265 ISMN stations were utilized, with the majority located in the United States and others distributed across Europe and Africa. Given that the highest station density occurs in the U.S. region, Figure R2b primarily highlights the distribution of ISMN stations in that area.

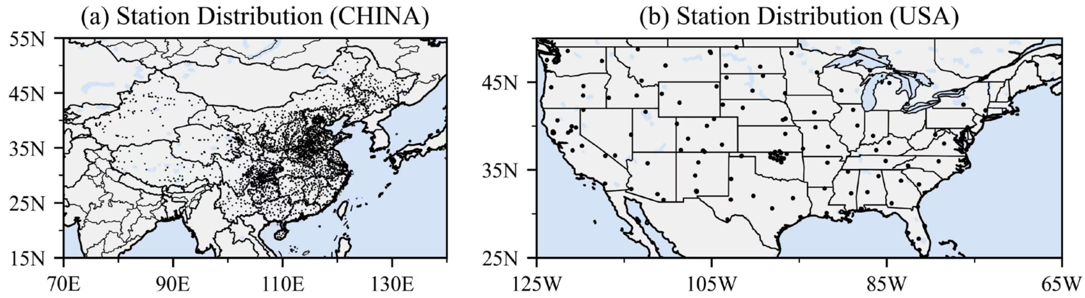

Figure R2: Spatial distribution of the in-situ soil moisture stations. (a) China Meteorological Administration network, and (b) International Soil Moisture Network stations located in the United States.

1.5 It is unclear which SMAP product is used. Line 107 states that the L2_SM_P_E product is used and the reference for this product is given, but line 108 states that the 36-km product is used. Please clarify.

Response:

We apologize for the lack of clarity in our original description. We revised the description of the SMAP product. The revised text can be found in Lines 184–187 of the revised manuscript, as follows:

Although the native spatial resolution of the radiometer is approximately 36 km, this enhanced product utilizes the Backus-Gilbert optimal interpolation technique to be distributed at a spatial sampling of 9 km on the EASE-Grid 2.0 projection.

2. One of the main findings from this paper is that the optimal combination of satellite sensors used in the assimilation is dependent on the observing conditions, specifically the vegetation density, which impact the uncertainty of the assimilated products. The authors address this by introducing an adaptive framework whereby the combination of satellite sensors changes depending on the vegetation density. However, in a traditional Kalman filter DA system, this sort of adaptive weighting of the impact of different observations is controlled through the observation error and its impact on the Kalman

gain. So, I wonder whether a cleaner implementation would be to use spatially and temporally varying observation errors for the three satellite products, which presumably would also reduce the impact of the X-band observations over densely vegetated areas. However, in the current manuscript it is unclear how the observation errors were characterized for the three satellite products or why the vegetation adaptive scheme was chosen instead. Addressing these two questions would greatly strengthen this paper.

Response:

Thanks for your suggestions. Following your suggestions, we have added a discussion on the applicability of error adjustment and the necessity of its variation with vegetation screening. The corresponding revision can be found in Lines 155–161 of the revised manuscript. The revised text is as follows:

"Although adjusting observation weights based on error estimation results can reduce the negative influence of highly uncertain data on assimilation performance, the relatively large errors associated with X-band products indicate that their observations may exhibit comparatively large deviations. Even when assigned small weights, such observations may still lead to degraded assimilation performance. This issue is more evident in global land data assimilation. Therefore, effectively integrating X-band retrieval products with those from other frequency bands and achieving stable improvements in global land data assimilation remain key challenges for the assimilation of X-band products. "

3. The suitability of the chosen spin-up- approach is unclear, as the methodology section does not provide sufficient detail to fully assess it. The authors describe a 342--year spin-up prior to the -two-month experiment period, but it is not clear whether this spin-up was conducted separately for each experiment configuration. For example, in the L+C configuration, does the spin-up already include the assimilation of L+C observations? Or was the -spin-up performed as an -open loop run with no data assimilation? If the latter is the case, then an additional -spin-up- period after activating the DA would be necessary to allow the system to adjust to the new configuration. The behavior shown in Figure 2, specifically the continuously increasing correlation values

and decreasing RMSE throughout the assimilation period, suggests that the system may indeed have been initialized from a no DA -spin-up-and was still adjusting during the experiment period.

Response:

Thanks for your suggestions. Following your suggestions, we further examined the possible influence of spin-up on the assimilation evaluation.

To provide a more objective assessment, we analyzed the assimilation results after excluding the initial adjustment period. As shown by the temporal evolution of the spatial correlation coefficient of surface soil moisture (Figure 2), the system reaches a quasi-steady state within approximately 8 days after assimilation is activated. Based on this, we computed the evaluation metrics for both the full assimilation period (Days 1–61) and the period excluding the initial adjustment (Days 8–61). As shown in Figure R3, the results from these two periods are highly consistent. The relative improvements across different frequency-band assimilation experiments remain nearly unchanged, regardless of whether the initial adjustment period is included. This indicates that, although the absolute performance is influenced by spin-up, the comparative conclusions regarding the relative performance of different frequency bands are robust. Figure R3 has been added to the Supplement as Figure S2.

To clarify this issue, we have added the following statement in the revised manuscript (Lines 361–363):

"This spin-up was run entirely in open loop, with all assimilation experiments starting from the same open-loop initial conditions rather than from a separate assimilation spin-up."

We have also added the following clarification in the discussion section (Lines 795–798):

"Because no independent data assimilation spin-up was available, the system undergoes a transient adjustment after DA is activated. Surface soil moisture reaches a quasi-steady state within about 8 days, and the results for Days 1-61 are highly consistent with those for Days 8-61. This consistency indicates that the initial adjustment does not affect the main conclusion regarding the relative assimilation skill of the different microwave bands."

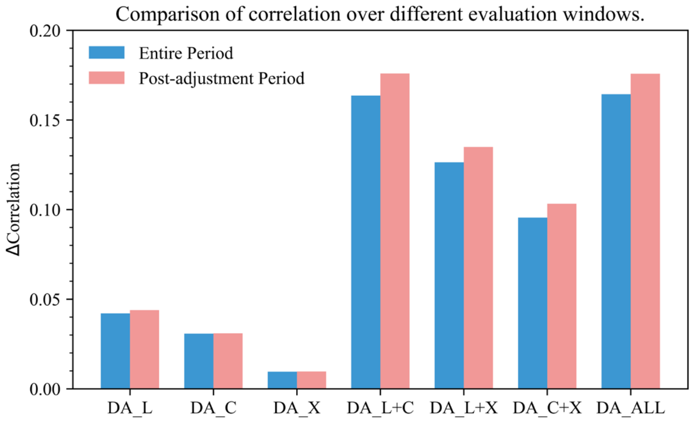

Figure R3: Comparison of assimilation performance over two evaluation windows: the full period (Days 8–61) and the post-adjustment period (Days 10–61). The bar chart illustrates the mean correlation coefficient differences between the assimilation experiments and the CTL, based on in situ observations.

4. Generally, the experiment period of 2 months seems much too short. It does not capture any seasonal or interannual effects and raises questions about the transferability of the conclusions drawn here to other parts of the year. I invite the authors to provide a rationale for choosing such a short experiment period (is it limited by data availability?) and consider extending the period if possible.

Response:

Thank you for your suggestions. Following your suggestions, we have extended the assimilation experiments to cover all four seasons of the year (Spring MAM, Summer JJA, Autumn SON, and Winter DJF). Results from other seasons also support our conclusion. The key to achieving positive results with X-band lies in selecting X-band products with smaller observational errors. Indeed, as the reviewer pointed out, seasonal variations affect the selection of X-band data. Through the comparative analysis of multi-season assimilation performance, we found that, in addition to vegetation type, the seasonal variation of vegetation should also be considered when assessing the impact of X-band assimilation.

We have added the relevant analysis to Figures 18 and 19 in Lines 723-766 of the revised manuscript, where Figure 18 shows the seasonal assimilation performance for representative vegetation types and Figure 19 presents the seasonal probability density distributions of the correlation coefficient differences among different assimilation experiments. The revised text is as follows:

To further investigate the differences in assimilation results across seasons, we extended the experiments to include spring (MAM), autumn (SON), and winter (DJF). Figure R4 presents a comparison of the correlation coefficients between the DA_L+C and DA_ALL experiments across the four seasons for different vegetation types. The Non-arctic Grass and Corn regions exhibit more pronounced seasonal differences. In summer (JJA) and winter (DJF), the growth of grasses and crops tends to stabilize, or the vegetation density decreases significantly. As a result, observation errors are relatively stable, making the addition of the X-band more likely to result in positive effects. As shown in the figure, the orange bars are noticeably higher than the blue bars during summer and winter.

Conversely, during the transitional phases of spring (MAM) and autumn (SON), the orange bars are lower than the blue bars, indicating that the inclusion of X-band data degrades the overall assimilation performance. This is likely because vegetation undergoes rapid growth or senescence during spring and autumn, accompanied by drastic changes in morphological structure and water content. As a result, X-band observations, which are more sensitive to vegetation effects, are more strongly influenced under these conditions. When vegetation dynamics are not adequately represented, soil moisture retrievals may exhibit increased variability and occasional anomalous estimates, thereby increasing observation errors (Dash and Sinha, 2019; Stradiotti et al., 2025). This elevated error uncertainty causes the assimilation of X-band data to be prone to negative impacts.

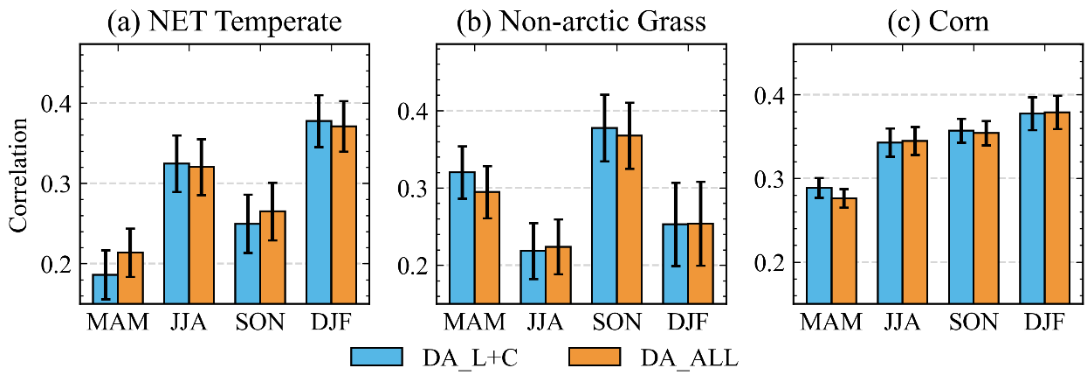

Figure R4: Comparison of assimilation performance for representative vegetation types across different seasons. The figure shows the correlation coefficients between simulated soil moisture and station observations for (a) NET Temperate, (b) Non-arctic Grass, and (c) Corn across the four seasons. The blue and orange bars represent the DA_L+C and DA_ALL experiments, respectively. Error bars indicate the 95% confidence intervals.

Based on the above analysis, the winter settings follow those of summer, where X-band data is excluded only in dense vegetation areas. In spring and autumn, X-band data is not introduced in Corn and Non-arctic Grass. This is because Cron and Non-arctic Grass are undergoing rapid growth or senescence during the transitional phases of spring and autumn. The resulting substantial changes in vegetation morphology and water content are prone to enhancing X-band scattering noise and increasing observation uncertainty.

Figure R5 displays the PDF of the differences in correlation coefficients between the three sets of assimilation experiments and the control experiment based on in situ observations. As shown in Figure R5, the differences for all assimilation experiments are primarily distributed in the range greater than zero, indicating that assimilating satellite data produces a positive effect. The probability distribution of these differences reveals that improvements are more likely to occur during spring and autumn, where the probability of a correlation coefficient increment exceeding 0.5 is higher than in the other two seasons. In contrast, the assimilation improvement in winter is relatively small, with the magnitude of correlation coefficient increments mainly concentrated around 0.1.

Comparing the improvement effects of different assimilation experiments, it is evident that the DA_NEW experiment reduces the probability of negative effects across all seasons, shifting the overall probability density distribution toward the positive effect interval. Compared with the DA_ALL experiment, the improvements of the new scheme in spring, summer, and autumn are more concentrated around 0.3, while in winter, they are concentrated around 0.1. Furthermore, the mean correlation coefficients for each season indicate that the DA_NEW experiment produces higher average values than both the DA_L+C and DA_ALL experiments in every season. This demonstrates that the new scheme, by dynamically adjusting the combination of multi-source data, better integrates the advantages of multi-source observations, thereby improving global land surface assimilation performance.

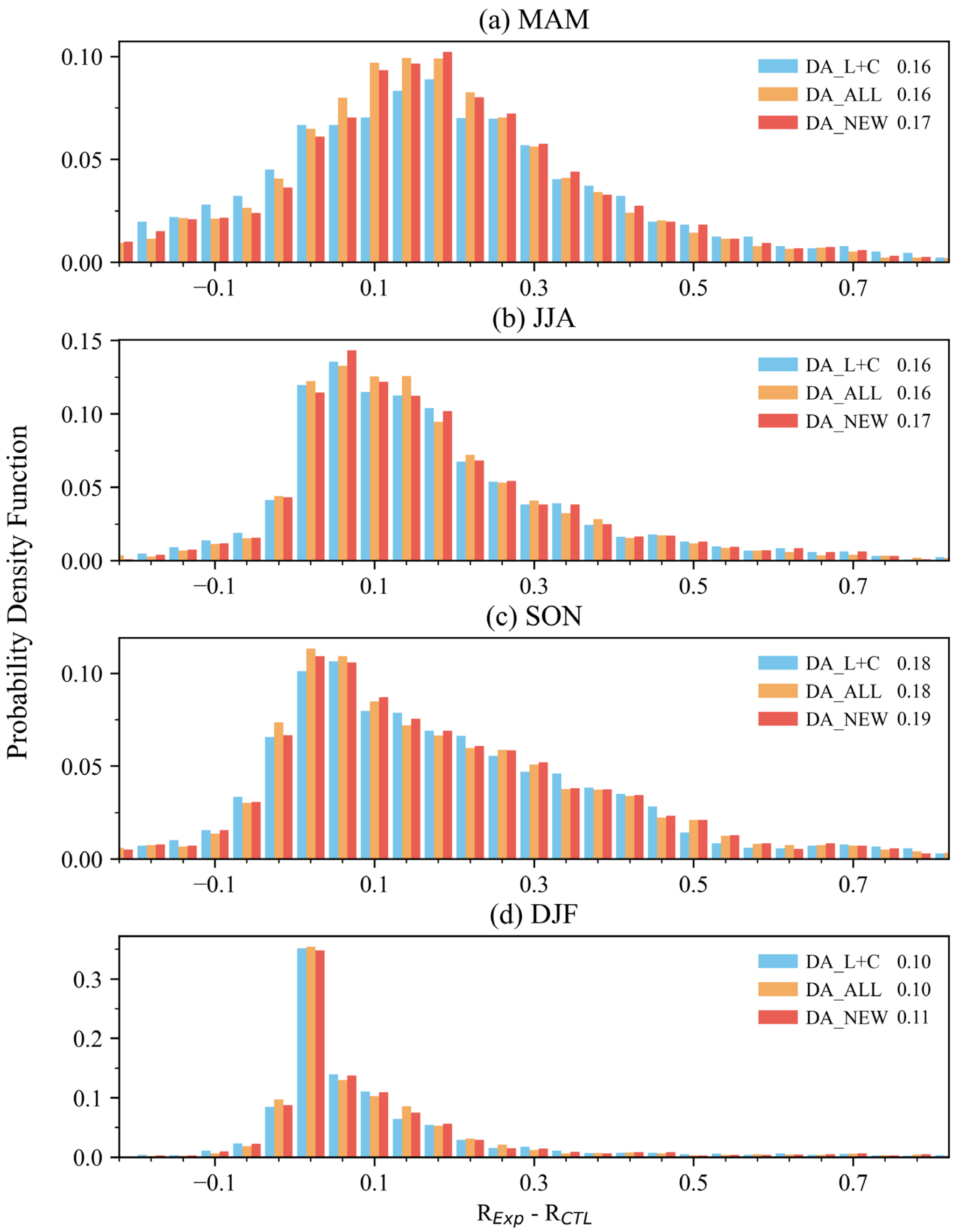

Figure R5: Seasonal variations in the probability density functions of the correlation coefficient differences between the assimilation experiments (DA_L+C, DA_ALL, and DA_NEW) and the control experiment based on station observations. (a) Spring (MAM), (b) Summer (JJA), (c) Autumn (SON), and (d) Winter (DJF). The numbers in the upper-right corner indicate the mean values.

The following references have been added to the reference part of the revised manuscript:

Dash, S. K. and Sinha, R.: A Comprehensive Evaluation of Gridded L-, C-, and X-Band Microwave Soil Moisture Product over the CZO in the Central Ganga Plains, India, Remote Sensing, 14, 1629, https://doi.org/10.3390/rs14071629, 2019.

Stradiotti, P., Gruber, A., Preimesberger, W., and Dorigo, W.: Accounting for seasonal retrieval errors in the merging of multi-sensor satellite soil moisture products, Science of Remote Sensing, 12, 100242, https://doi.org/10.1016/j.srs.2025.100242, 2025.

5. For the global evaluation, ERA5-Land is used as a reference. However, ERA5-Land is forced with meteorological fields from ERA5, which does assimilate ASCAT soil moisture observations. So, there is an indirect influence from ASCAT soil moisture retrievals on the ERA5-Land soil moistures. Also, the CoLM model is forced with ERA5 meteorological fields that are impacted by the ASCAT SM assimilation. It is possible that the very good performance of the C-band data assimilation in Figure 2 is a side effect of this? I would suggest to either use a more independent reference for the global evaluation or to at least discuss the possible impact of ASCAT.

Response:

Thanks for your suggestions. Following your suggestions, we clarified the potential indirect influence of ASCAT observations on ERA5-Land in the revised manuscript. To complement the ERA5-Land-based global evaluation, we also assessed the assimilation results using independent in situ soil moisture observations from the ISMN and CMA networks, as shown in Figures 6 and 7. These ground-based observations are independent of both ERA5-Land and ASCAT, and the results consistently support the conclusions drawn from the global evaluation.

The corresponding clarification can be found in Lines 411–414 of the revised manuscript. The added text is as follows:

It should be noted that ERA5-Land is an offline simulation driven by ERA5 atmospheric forcing. Because ERA5 itself has already assimilated ASCAT soil moisture data, this indirect coupling implies that the validation process is not strictly independent. This relationship might lead to an overestimation of the skill scores for ASCAT to some degree.

Minor Comments:

1. The naming convention in the plots is all over the place. The assimilation experiments are sometimes referred to as 'L', 'C', and 'X', sometimes as 'SMAP', 'ASCAT', and 'MWRI', sometimes as 'DA_L', 'DA_C', and 'DA_X'. The X-band experiments are referred to as 'X', 'DA_X', 'MWRI, or 'FY3D' depending on the plot. Please make sure you pick one naming convention and use it consistently throughout. I would also suggest using different names/label when you are evaluating data assimilation experiments and when you are evaluating retrievals.

Response:

Thanks for your suggestions. Following your suggestions, we revised the figure captions, experiment names, and related descriptions throughout the manuscript to improve consistency and readability. The main revisions are as follows:

1. All data assimilation experiments are now consistently labeled as DA_L, DA_C, and DA_X in the revised manuscript, corresponding to the assimilation of L-band (SMAP), C-band (ASCAT), and X-band (MWRI) soil moisture products, respectively.

2. For the evaluation of the satellite retrieval products themselves, we consistently use the sensor names (e.g., SMAP, ASCAT, and MWRI) to distinguish them clearly from the assimilation experiment labels.

2. The differences between the various experiments are often very small. For the bar graphs, I would suggest including confidence intervals (or some other measure of significance) as well as some indication of the number of stations used in the evaluation against the in situ data.

Response:

Thanks for your suggestions. Following your suggestions, we have added 95%

confidence intervals to the bar charts. In addition, the number of stations used in the evaluation against the in-situ data has been included in the figures. These revisions have been applied to Figures 5, 6, 7, and 9.

3. Please include more detail regarding the satellite data that are being used. I would suggest including the data period of each sensor, the spatial resolution, the revisit time, the temporal resolution of the satellite product, and the retrieval approach used.

Response:

Thanks for your suggestions. Following your suggestions, we expanded Section 2.1 "Satellite datasets" by adding key technical information on the satellite retrieval products used in this study. The added description includes the data period, operating frequency bands, spatial resolution or spatial sampling, revisit time, temporal resolution of the products, and retrieval algorithms. The added text can be found in Lines 178–209 of the revised manuscript, as follows:

This study utilized the Soil Moisture Active Passive (SMAP) Level-2 Enhanced Passive Soil Moisture product (L2_SM_P_E) provided by the U.S. National Snow and Ice Data Center (NSIDC) (O'Neill et al., 2023). Launched in January 2015, the SMAP satellite has been continuously providing global radiometer observations since April 2015. It operates in a sun-synchronous orbit with an L-band (1.41 GHz) radiometer. The descending and ascending overpasses occur at approximately 6:00 AM and 6:00 PM Local Solar Time, respectively, yielding a global revisit time of 2–3 days. Based on the well-validated $\tau-\omega$ radiative transfer model, this product implements both the Single Channel Algorithm using vertical polarization (SCA-V) and the Dual Channel Algorithm (DCA) for soil moisture retrieval (Chaubell et al., 2020; O'Neill et al., 2021). The characteristics of the L-band provide it with canopy penetration capabilities. Although the native spatial resolution of the radiometer is approximately 36 km, this enhanced product utilizes the Backus-Gilbert optimal interpolation technique to be distributed at a spatial sampling of 9 km on the EASE-Grid 2.0 projection.

The ASCAT retrieval data are derived from the Advanced Scatterometer onboard the MetOp-C satellite operated by the European Organization for the Exploitation of

Meteorological Satellites (EUMETSAT). Following its launch in November 2018, MetOp-C has continuously provided high-quality global data, extending the long-term ASCAT data record. The satellite has equatorial crossing times of approximately 9:30 AM (descending) and 9:30 PM (ascending), providing a global revisit time of about 3 days. As an active microwave radar operating at the C-band (5.255 GHz, VV polarization), ASCAT provides global soil moisture estimates by measuring the surface radar backscatter coefficient (σ^0). This study utilizes the ASCAT Level 2 Surface Soil Moisture product (EO:EUM:DAT:METOP:SOMO12) at 12.5 km spatial sampling on the swath grid. The temporal resolution of this product relies on daily morning and evening discrete observations. Regarding the retrieval algorithm, this product is based on the TU Wien change detection algorithm, obtaining relative soil moisture, which is expressed as a degree of saturation percentage from 0 to 100%, by linearly scaling the backscatter coefficient between historical dry and wet reference lines (Bartalis et al., 2007). Subsequently, this study utilizes soil porosity data provided by the European Space Agency Climate Change Initiative (ESA-CCI) to convert this saturation into volumetric soil water content.

The MWRI soil moisture dataset was developed by the National Satellite Meteorological Center (NSMC) of the China Meteorological Administration (CMA). The FY-3D afternoon satellite was successfully launched in November 2017, with its MWRI data record officially available since early 2018. The dataset is derived from global passive microwave brightness temperature observations acquired by the MWRI instrument onboard FY-3D, which has equatorial crossing times of approximately 2:00 AM (descending orbit) and 2:00 PM (ascending orbit), providing a global revisit time of 1–2 days. Surface soil moisture is primarily retrieved from the X-band (10.65 GHz) dual-polarized brightness temperatures using a parameterized Q_p emission model that accounts for vegetation scattering, optical depth, and soil surface roughness effects (Kang et al., 2020). This daily product combines ascending and descending overpasses and is provided on a 25 km Equal-Area Scalable Earth (EASE-Grid) projection.

The following references have also been added to the revised manuscript:

Chaubell, M. J., Yueh, S. H., Dunbar, R. S., Colliander, A., Chen, F., Chan, S. K., Entekhabi, D., Bindlish, R., O'Neill, P. E., Asanuma, J., Berg, A. A., Bosch, D. D., Caldwell, T., Cosh, M. H., Holifield Collins, C., Martínez-Fernández, J., Seyfried, M., Starks, P. J., Su, Z., Thibeault, M., and Walker, J.: Improved SMAP dual-channel algorithm for the retrieval of soil moisture, IEEE Trans. Geosci. Remote Sens., 58, 3894–3905, https://doi.org/10.1109/TGRS.2019.2959239, 2019.

O'Neill, P. E., Bindlish, R., Chan, S., Chaubell, J., Colliander, A., Njoku, E., and Jackson, T.: Soil Moisture Active Passive (SMAP) Algorithm Theoretical Basis Document: Level 2 & 3 Soil Moisture (Passive) Data Products, Revision G, Jet Propulsion Laboratory, California Institute of Technology, JPL D-66480, 111 pp., 2021.

The following references are cited here and were already included in the original manuscript:

Bartalis, Z., Wagner, W., Naeimi, V., Hasenauer, S., Scipal, K., Bonekamp, H., Figa, J., and Anderson, C.: Initial soil moisture retrievals from the METOP-A Advanced Scatterometer (ASCAT), Geophys. Res. Lett., 34, https://doi.org/10.1029/2007GL031088, 2007.

Kang, C. S., Zhao, T., Shi, J., Cosh, M. H., Chen, Y., Starks, P. J., Collins, C. H., Wu, S., Sun, R., and Zheng, J.: Global Soil Moisture Retrievals from the Chinese FY-3D Microwave Radiation Imager, IEEE Trans. Geosci. Remote Sens., 59, 4018–4032, https://doi.org/10.1109/TGRS.2020.3019408, 2020.

O'Neill, P., Chan, S., Njoku, E., Jackson, T., Bindlish, R., Chaubell, J., and Colliander, A.: SMAP enhanced L2 radiometer half-orbit 9 km EASE-grid soil moisture, version 6, https://doi.org/10.5067/BN36FXOMMC4C, 2023.

4. Each of the retrieval algorithms used the generate the products used here makes assumptions about the observing conditions, such as the vegetation state or the soil temperature. That means that to some extent differences in the performance observed here could be due to assumptions about for example the vegetation state made by one retrieval algorithm matching better with the vegetation state in the reference data. These effects can be limited by assimilating radiances instead of retrieval products. Could you please comment in the text why you chose to assimilate retrieval products rather than satellite radiances?

Response:

Thanks for your suggestions. Indeed, as the reviewer pointed out, Direct assimilation of radiances can reduce the uncertainty associated with retrieval errors and is indeed an important direction for the future development of land data assimilation. Considering that X-band assimilation is relatively rare, we first aimed to demonstrate its value by assimilating X-band retrieval products. Following your suggestion, we have added the following discussion in Lines 210-213.

We selected X-band retrieval products because X-band applications remain relatively limited, and we aimed to demonstrate their value through direct assimilation. Direct assimilation of radiances is certainly an important direction for land surface data assimilation. However, it requires a reasonable estimation of the errors in simulations from the radiative transfer model. This aspect warrants further investigation in future studies.

5. Please include units and colorbar labels on the plots where they are missing.

Response:

Thanks for your suggestions. Following your suggestions, we checked all relevant figures throughout the manuscript and added the missing physical units and colorbar labels (e.g., the soil moisture unit, m^3/m^3). We also reviewed the numerical ranges and tick labels of the colorbars to ensure that the variables and their units are presented clearly and consistently across the figures. These revisions have been made in Figures 1, 2, 4, 5, 6, 7, 9, 12, and 13.

Detailed Comments:

1. l.18 "significantly improves" Including confidence intervals as suggested above would help support this claim.

Response:

Thanks for your suggestions. We have added 95% confidence intervals to the relevant bar charts and indicated the number of stations used in each comparison. These revisions have been incorporated into Figures 5, 6, 7, and 9. In addition, we have revised the statement to ensure consistency with the statistical evidence presented in the figures and to avoid overstatement.

The original sentence: "Results show that assimilating soil-moisture retrievals significantly improves the accuracy of the CoLM land-surface model; nevertheless, the effectiveness of each product exhibits a pronounced dependency on vegetation type." has been revised to (Lines 18–19): "Results show that assimilating soil-moisture retrievals improves the accuracy of the CoLM land-surface model; nevertheless, the effectiveness of each product varies with vegetation type."

2. l.25 "rises by about 0.25". Is this compared to the open loop? Please specify.

Response:

Thanks for your suggestions. Following your suggestions, we added the phrase "compared with the open-loop simulation" in the Abstract to clarify that the reported increase in the correlation coefficient is relative to the open-loop simulation. The corresponding revision can be found in Lines 24–25 of the revised manuscript.

3. ll.57-59: SMAP only provided active and passive data in its original configuration for a few months (until the failure of the radar). If you are referring to the SMAP/Sentinel product here, please include the appropriate reference.

Response:

Thanks for your suggestions. We are using SMAP products, not SMAP/Sentinel products. The revised text can be found in Lines 62–63 of the revised manuscript, as follows:

However, its active radar ceased operations on 7 July 2015, a few months after launch, leaving its L-band passive radiometer as the primary instrument for ongoing soil moisture products.

4. l.63 Draper and Reichle 2015 uses GEOS/Catchment, not SiB2. Please adjust the text or include the appropriate reference for SiB2.

Response:

We apologize for the inaccurate citation in the original manuscript. Following your suggestions, we state that their study employed the GEOS/Catchment model. We also checked the other references throughout the manuscript to improve citation accuracy.

5. ll.66-69: For the discussion of the SMAP data assimilation I suggest also including the discussion of the SMAP Level-4 SM (data assimilation) product that is part of the

official product suite (Reichle et al., 2019), as well as studies that have investigated the impact of SMAP DA in NWP systems (e.g., Carrera et al, 2019)

Reichle, R.H., Liu, Q., Koster, R.D., Crow, W.T., De Lannoy, G.J., Kimball, J.S., Ardizzone, J.V., Bosch, D., Colliander, A., Cosh, M. and Kolassa, J., 2019. Version 4 of the SMAP level-4 soil moisture algorithm and data product. Journal of Advances in Modeling Earth Systems, 11(10), pp.3106-3130.

Carrera, M.L., Bilodeau, B., Bélair, S., Abrahamowicz, M., Russell, A. and Wang, X., 2019. Assimilation of passive L-band microwave brightness temperatures in the Canadian land data assimilation system: Impacts on short-range warm season numerical weather prediction. Journal of Hydrometeorology, 20(6), pp.1053-1079.

Response:

Thanks for your suggestions. Following your suggestions, we expanded the discussion of previous SMAP assimilation studies in the Introduction, including the work by Reichle, Carrera, and Tian. The revised text can be found in Lines 70–75 of the revised manuscript, as follows:

The official SMAP Level-4 soil moisture product provides a continuous global dataset by assimilating SMAP brightness temperatures into the Catchment land surface model (Reichle et al., 2019). This assimilation approach has also proven effective in numerical weather prediction. For example, Carrera et al. (2019) assimilated SMAP L-band brightness temperatures into the Canadian Land Data Assimilation System (CaLDAS) and reported clear improvements in short-range warm-season forecasts, particularly for 2-m dewpoint temperatures. Tian et al. (2023) demonstrated that assimilation of SMAP products not only enhanced land surface model forecasts but also improved parameter estimation.

6. l.72 "long revisit periods" This is really only true for SAR or other high-resolution sensors.

Response:

Thanks for your suggestions. Following your suggestions, we revised the relevant paragraph in the Introduction to provide a clearer description of the characteristics of different microwave sensors, especially the classification within active microwave sensors. The revised text distinguishes among SAR products, ASCAT products, and SMAP products, and further clarifies their differences in spatial resolution and temporal coverage. The corresponding revision can be found in Lines 81–88 of the revised manuscript. The revised text is as follows:

"Depending on the instrument bands and orbital characteristics, the strengths and weaknesses of various soil moisture products differ significantly. Passive microwave products offer excellent temporal coverage but suffer from coarse spatial resolution. Conversely, while Synthetic Aperture Radar (SAR) products provide high spatial resolution, their temporal coverage is limited. The Scatterometer (ASCAT) strikes a balance with high temporal coverage and moderate resolution, while L-band active-passive combined instruments, such as SMAP, attempt to integrate the advantages of all three. Although continuous advancements in retrieval algorithms have led to marked improvements in the accuracy of soil moisture products across all instrument types, vegetation density continues to exert a significant influence on the product precision of instruments operating in different frequency bands."

The following references have been added to the reference part of the revised manuscript:

Carrera, M. L., Bélair, S., and Bilodeau, B.: Assimilation of passive L-band microwave brightness temperatures in the Canadian Land Data Assimilation System: Impacts on short-range warm season numerical weather prediction, J. Hydrometeor., 20, 1085–1105, https://doi.org/10.1175/JHM-D-18-0133.1, 2019.

Reichle, R. H., Liu, Q., Koster, R. D., Crow, W. T., De Lannoy, G. J. M., Kimball, J. S., Ardizzone, J. V., Bosch, D., Colliander, A., Cosh, M., Kolassa, J., Mahanama, S. P., Prueger, J., Starks, P., and Walker, J. P.: Version 4 of the SMAP Level-4 Soil Moisture Algorithm and Data Product, J. Adv. Model. Earth Syst., 11, 3106–3130, https://doi.org/10.1029/2019MS001729, 2019.

The following references are cited here and were already included in the original manuscript:

Tian, J., Lu, H., Yang, K., Qin, J., Zhao, L., Zhou, J., Jiang, Y., and Ma, X.: Quick estimation of parameters for the land surface data assimilation system and its influence based on the extended Kalman filter and automatic differentiation, Sci. China Earth Sci., 66, 2546–2562, https://doi.org/10.1007/s11430-022-1180-8, 2023.

7. l.75 "L-band missions (SMOS, SMAP) penetrate vegetation well" They penetrate

vegetation better, but L-band sensors also have difficulties "seeing" the surface under dense vegetation (VWC > 5 kg/m^2)

Response:

Thanks for your suggestions. Following your suggestions, we revised the description of L-band sensors to clarify both their penetration capability and their limitations under dense vegetation conditions. The corresponding revision can be found in Lines 97–100 of the revised manuscript. The revised text is as follows:

"Compared with high-frequency bands, L-band sensors such as SMOS and SMAP possess superior physical penetration capabilities, which allow them to effectively penetrate the vegetation canopy and acquire soil information. However, in regions with dense vegetation cover, specifically when the vegetation water content (VWC) exceeds 5 kg/m^2, the capacity to effectively retrieve surface information remains significantly limited (Entekhabi et al., 2010; Kerr et al., 2010)."

The following references are cited here and were already included in the original manuscript:

Entekhabi, D., Njoku, E. G., O'Neill, P. E., Kellogg, K. K., Crow, W. T., Edelstein, W. N., Entin, J. K., Goodman, S. D., Jackson, T. J., Johnson, J., Kimball, J., Piepmeier, J. R., Koster, R. D., Martin, N., McDonald, K. C., Moghaddam, M., Moran, S., Reichle, R., Shi, J. C., Spencer, M. W., Thurman, S. W., Tsang, L., and Van Zyl, J.: The Soil Moisture Active Passive (SMAP) mission, Proc. IEEE, 98, 704–716, https://doi.org/10.1109/JPROC.2010.2043918, 2010.

Kerr, Y. H., Waldteufel, P., Wigneron, J. P., Delwart, S., Cabot, F., Boutin, J., Escorihuela, M. J., Font, J., Reul, N., Gruhier, C., Juglea, S. E., Drinkwater, M. R., Hahne, A., Martin-Neira, M., and Mecklenburg, S.: The SMOS mission: New tool for monitoring key elements of the global water cycle, Proc. IEEE, 98, 666–687, https://doi.org/10.1109/JPROC.2010.2043032, 2010.

8. ll.83-86: The statements made in this section are not quite accurate. There are plenty of studies that have investigated the synergistic assimilation of soil moisture from different sensors, for example:

Draper, C.S., Reichle, R.H., De Lannoy, G.J.M. and Liu, Q., 2012. Assimilation of passive and active microwave soil moisture retrievals. Geophysical Research Letters, 39(4).

Lievens, H., Reichle, R.H., Liu, Q., De Lannoy, G.J., Dunbar, R.S., Kim, S.B., Das, N.N., Cosh, M., Walker, J.P. and Wagner, W., 2017. Joint Sentinel-1 and SMAP data assimilation to improve soil moisture estimates. Geophysical research letters, 44(12), pp.6145-6153.

Girotto, M., Reichle, R.H., Rodell, M., Liu, Q., Mahanama, S. and De Lannoy, G.J., 2019. Multi-sensor assimilation of SMOS brightness temperature and GRACE terrestrial water storage observations for soil moisture and shallow groundwater estimation. Remote Sensing of Environment, 227, pp.12-27.

Additionally, there are many studies investigating the complementary synergy of different satellite retrieval products, for example in the context of the ESA-CCI project. Finally, the studies that are cited here do indeed investigate the complementarity of different sensors. I suggest rewriting this section to acknowledge the existing body of work, whilst also highlighting the novel contributions from this study (e.g., the inclusion of X-band data).

Response:

Thanks for your suggestions. Following your suggestions, we added a discussion of previous multi-satellite soil moisture assimilation and merging studies, and further clarified the specific contribution of our study.

In the revised manuscript, we added a discussion of previous studies on the integration of observations from different satellites. The corresponding revision can be found in Lines 116–121 of the revised manuscript. The revised text is as follows:

"Draper et al. (2012) assimilated passive and active microwave soil moisture retrievals and reported improved estimates. Lievens et al. (2017) further combined SMAP and Sentinel-1 observations and found that the joint assimilation scheme performed best. Girotto et al. (2019) assimilated SMOS brightness temperatures together with GRACE observations, improving estimates of soil moisture, groundwater, and runoff. The ESA-CCI project has likewise explored the integration of multiple satellite retrieval products to generate more consistent and higher-quality global datasets, primarily through the development of dynamic weighting schemes based on Triple Collocation (TC) error variance estimation (Dorigo et al., 2017; Gruber et al., 2019). "

We also clarified the research background and motivation for incorporating X-band retrieval products into multi-satellite data assimilation. The corresponding revision can be found in Lines 123–129 of the revised manuscript. The revised text is as follows:

"Although data assimilation integrating observations from multiple satellites has received increasing attention, relatively few studies have focused on multi-satellite assimilation that explicitly incorporates X-band observations. China has launched several Fengyun-3 (FY-3) polar-orbiting meteorological satellites. Among the currently operating FY-3 satellites, FY-3D, FY-3F, FY-3G, and FY-3H carry microwave imagers, including MWRI/MWRI-II and MWRI-RM, with X-band channels, providing abundant retrieval products derived from X-band microwave observations. Therefore, how to effectively integrate X-band products with products from other frequency bands remains an important research direction that requires further investigation. "

We further clarified the main contribution of our study by emphasizing the specific challenge of achieving stable improvements when assimilating X-band retrieval products together with products from other frequency bands in global land data assimilation. The corresponding revision can be found in Lines 155–161 of the revised manuscript. The revised text is as follows:

"Although adjusting observation weights based on error estimation results can reduce the negative influence of highly uncertain data on assimilation performance, the relatively large errors associated with X-band products indicate that their observations may exhibit comparatively large deviations. Even when assigned small weights, such observations may still lead to degraded assimilation performance. This issue is more evident in global land data assimilation. Therefore, effectively integrating X-band retrieval products with those from other frequency bands and achieving stable improvements in global land data assimilation remain key challenges for the assimilation of X-band products. "

9. l.93: The Kerr et al., 2010 reference is not about X-band sensors, so maybe not an appropriate reference here.

Response:

Thanks for your suggestions. Following your suggestions, Kerr et al. (2010) was moved to after the L-band, line 149. Jackson and Schmugge (1991) was moved to after the X-band, line 142. Owe et al. (2001) was moved to after the C-band, line 147.

10. l.151 Please include the citation for ERA5:

Hersbach H, Bell B, Berrisford P, et al. The ERA5 global reanalysis. Q J R Meteorol Soc. 2020; 146:1999–2049. https://doi.org/10.1002/qj.3803

Response:

Thanks for your suggestions. Following your suggestions, we have added the reference in Line 299.

11. ll.155-159: It is unclear to me whether this text refers to ERA5 or the CoLM. Please clarify.

Response:

Thanks for your suggestions. Following your suggestions, we have rewritten this paragraph in the revised manuscript (Lines 299–304). We have explicitly separated the description of the ERA5 forcing data from the physical execution process of the CoLM model, and provided clear subjects for each sentence. The specific revisions are as follows:

"A bilinear interpolation method was used to interpolate the ERA5 data from its original 0.25° horizontal resolution to a 1.4° **grid**. **The interpolated forcing data** have a temporal resolution of 3 hours and cover the period from January 1, 1979, to December 31, 2022. **For the model integration, the CoLM** employs an explicit finite-difference method with a time step of 30 minutes to ensure simulation stability and accuracy. **The model outputs**, which include soil temperature, moisture, surface fluxes, evapotranspiration, and runoff, provide the basis for subsequent data assimilation and evaluation."

12. l.167 Please also include de Rosnay et al., 2013 as a reference.

De Rosnay, P., Drusch, M., Vasiljevic, D., Balsamo, G., Albergel, C. and Isaksen, L.,

2013. A simplified extended Kalman filter for the global operational soil moisture analysis at ECMWF. Quarterly Journal of the Royal Meteorological Society, 139(674), pp.1199-1213.

Response:

Thanks for your suggestions. Following your suggestions, we have added the citation to de Rosnay et al. (2013) in Line 313.

13. l.196: Could you please include some motivation for conducting the assimilation once daily?

Response:

Thanks for your suggestions. Based on your suggestion, we have incorporated these motivations into the relevant assimilation design section of the revised manuscript (Lines 377–383). The specific revised text is as follows:

A once-daily assimilation cycle was used in this study. Soil moisture has clear temporal persistence, and its day-to-day variability can therefore be adequately represented at a daily update interval. This choice is also consistent with the temporal characteristics of the input products, since ASCAT and SMAP are instantaneous satellite retrievals, whereas the FY-3D MWRI product used here is a fused daily product without a specific observation time. Using a 24 h assimilation window thus provides a common framework for integrating the three datasets. In addition, a higher update frequency would markedly increase the computational burden of the SEKF, which requires perturbation integrations to estimate the Jacobian of the observation operator at each analysis step.

14. Figure 3. It is a bit difficult to see the differences between the different products. You could consider changing this figure to show the ERA5-Land soil moisture and then three maps showing the differences of the three DA experiments with respect to ERA5-Land. Please also include a label and units on the colorbar and change the title of the bottom right map to "ERA5-Land".

Response:

Thanks for your suggestions. Following your suggestions, we have revised the Figure 3. ERA5-Land soil moisture is now shown as the reference field, while the other three panels display the differences between each assimilation experiment and ERA5-Land. Variable labels and units have also been added to the color bars.

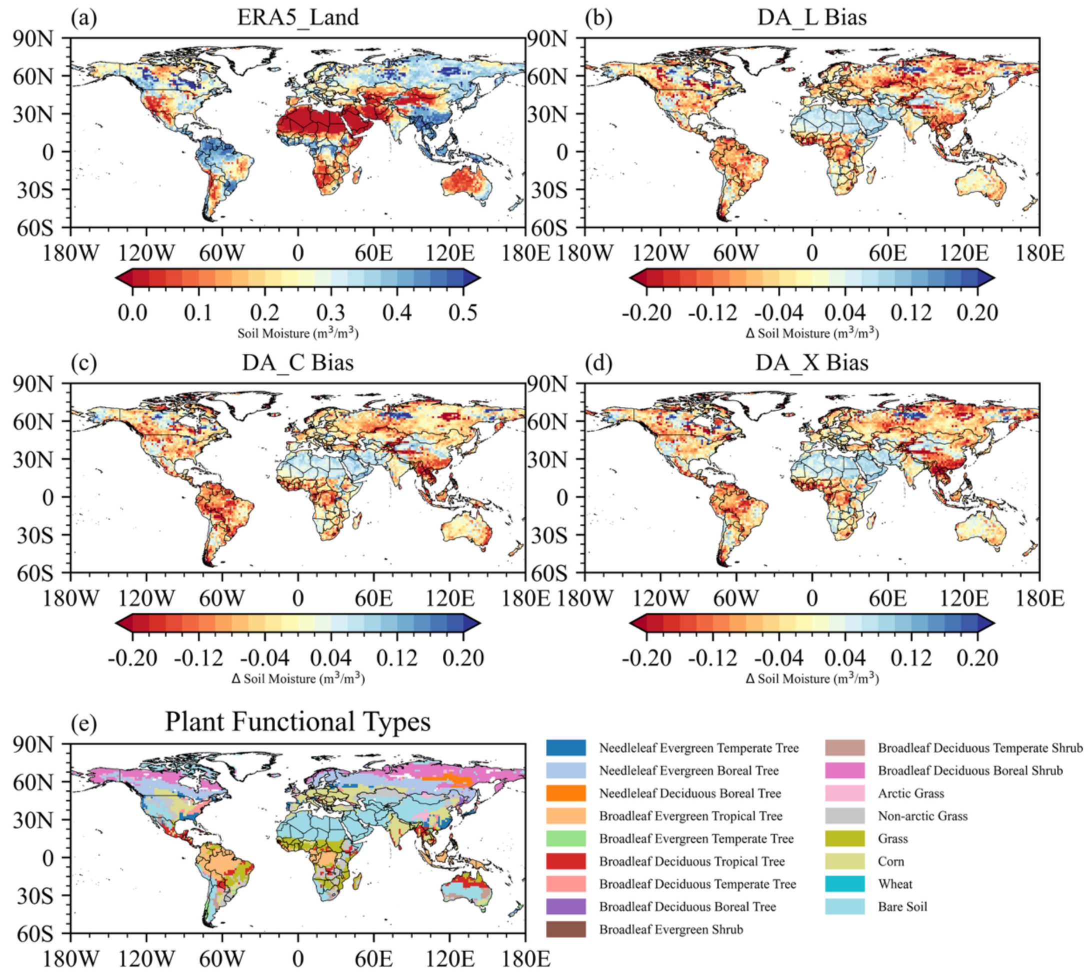

Figure R6: Spatial distribution of mean soil moisture in the top layer (0-7 cm) during 2 June to 3 July 2022. (a) shows the soil moisture from the ERA5_Land product. (b)–(d) show the soil moisture differences of the analysis fields from the DA_L, DA_C, and DA_X assimilation experiments relative to ERA5_Land, respectively (i.e., DA experiment minus ERA5-Land). (e) shows the spatial distribution of vegetation cover.

15. l.256: How was the vegetation density computed?

Figure 5: If these are organized according to increasing vegetation density, then why is "bare soil" not in the first slot? And since you are showing differences, please label the plots as ΔRMSE etc. (same for Figure 6).

Response:

Thanks for your suggestions. The ordering in Figure 5 is based on the average precipitation for each vegetation type. We added an explanation of the vegetation sorting method in Lines 469–470 of the revised manuscript: 'The vegetation types are sorted in ascending order based on the average precipitation of each region during the assimilation period.' We have uniformly updated all the y-axis labels in both figures to ΔRMSE and ΔCorrelation.

16. ll.269-270: Why did you choose not to include ISMN in this evaluation?

Response:

Thanks for your suggestions. We sincerely apologize for this oversight in the original manuscript. In fact, ISMN data have been consistently used in all subsequent validation and performance evaluations in this study. Accordingly, we have revised the sentence in the updated manuscript from: "Recognizing that reanalysis data are not absolute truth, we further evaluated the assimilation performance using in situ observations from China."

To the following: "Recognizing that reanalysis data are not absolute truth, we further evaluated the assimilation performance using in situ observations from China and the ISMN."

17. ll.286-288: I do not see the described behaviour in the plot. Could you please clarify what you mean?

Response:

We sincerely apologize for any confusion this caused. We have rewritten this paragraph in the revised manuscript (Lines 513–515) to accurately reflect our intent. The revised statement is as follows:

The retrieval accuracy of all three products exhibits a clear dependence on vegetation density. Owing to the stronger canopy penetration capability of L-band microwave radiometry, SMAP maintains relatively higher correlation and lower RMSE in densely vegetated areas compared to the other products.

18. ll.288-289: Qualitatively, ASCAT and SMAP seem to show a much more similar performance than ASCAT and MWRI.

Response:

Thanks for your suggestions. Following your suggestions, we expanded the relevant discussion to better reflect the evaluation results for ASCAT, SMAP, and MWRI under different vegetation conditions. The corresponding revision can be found in Lines 515–524 of the revised manuscript. The revised text is as follows:

ASCAT exhibits competitive overall performance relative to SMAP, owing partly to its robust time-series change detection algorithm. It tends to slightly outperform SMAP in low- and sparse-vegetation regions but performs marginally worse in moderate-to-high vegetation zones due to greater C-band signal attenuation. In contrast, the X-band MWRI product is notably inferior to both SMAP and ASCAT in moderately and densely vegetated areas owing to its shorter wavelength and limited penetration. Over sparsely vegetated and bare-soil regions, however, MWRI achieves accuracy that is comparable, or occasionally marginally superior, to the other two products. These results suggest that spatial variations in assimilation performance are primarily driven by the intrinsic differences in retrieval accuracy among the products. In summary, the relatively longer wavelengths of the L-band and C-band, combined with robust retrieval algorithms, enable SMAP and ASCAT to maintain high accuracy in vegetated areas, while the shorter X-band (MWRI) is more severely limited by vegetation-induced scattering and attenuation.

19. ll.297-304 I am not sure how you can draw these conclusions about the impact on forecast skill when you have not shown the forecast skill across different land cover or climate regions.

Response:

Thanks for your suggestions. We added Figure R7 to the revised manuscript as Figure 11, together with the related discussion, to illustrate how external forcing, particularly precipitation, can mask the impact of data assimilation. The corresponding revision can be found in Lines 537–548 of the revised manuscript. The added text is as follows:

Figure R7 illustrates the impact of precipitation on the persistence of assimilation increments. Figure R7a uses a typical BET Tropical grid point (6.38°N, 59.06°W) as an example to present the soil moisture time series. During the assimilation phase, continuous observational constraints result in a distinct divergence between the soil moisture sequences of the Data Assimilation (DA) experiment and the Control (CTL) experiment. However, in the forecast phase, external forcings such as heavy precipitation dominate the soil moisture state. This causes the DA and CTL simulation results to rapidly converge, which makes the information introduced via assimilation more susceptible to being masked. Figure R7b further demonstrates that densely vegetated regions, including BET Tropical and NET Temperate, typically experience higher average precipitation. Consequently, in these regions where the assimilation of L-band retrieval products otherwise performs relatively well, frequent and intense precipitation acts as an external forcing that quickly obscures the initial assimilation information, resulting in a more rapid decay in forecast skill.

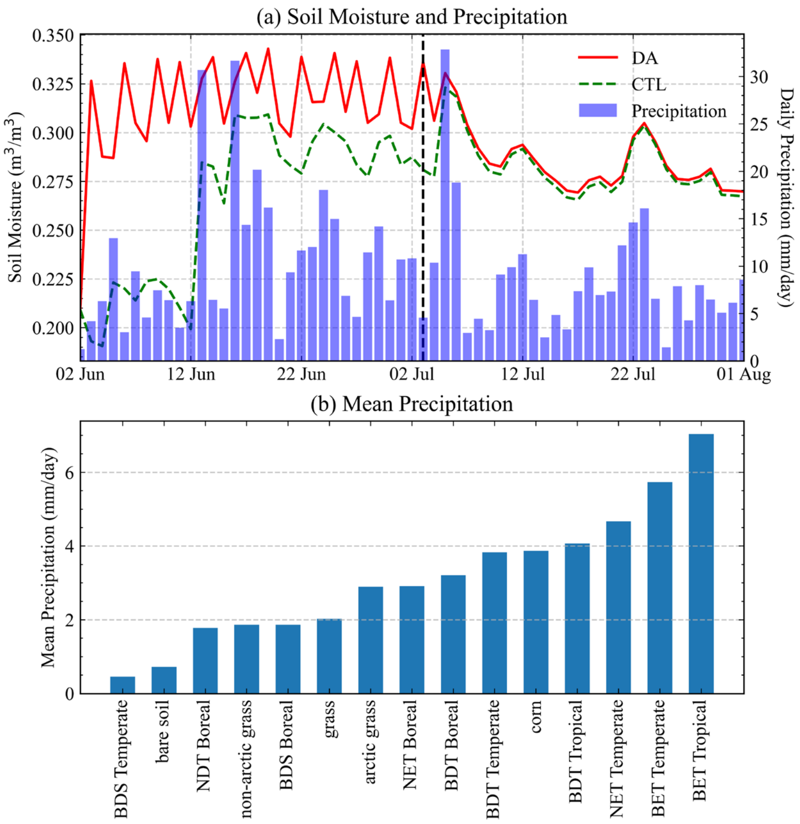

Figure R7: (a) Time series of daily precipitation and simulated soil moisture from the data assimilation (DA) and CTL experiments at a representative BET Tropical grid cell (6.38°N, 59.06°W). The vertical dashed line separates the assimilation phase and the forecast phase. (b) Mean precipitation across different vegetation types during the study period.

20. Figure 9: The y-axis label here is confusing. If I understand the text correctly, you are comparing the skill of a 3-sensor combination against the skill of a 2-sensor combination, not a single sensor. Please clarify this.

Response:

Thanks for your suggestions. We apologize for any confusion caused by the inaccurate labeling in Figure 9. In the revised manuscript, we have corrected the X-axis tick labels in Figure 9 to rectify the erroneous descriptions. The updated figure has been integrated into the text and is also provided here as Figure R8 for your convenience.

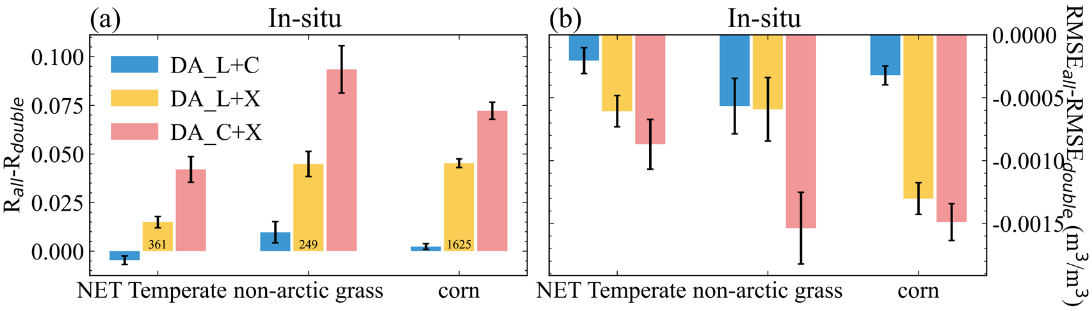

Figure R8: Changes in correlation coefficient (a) and RMSE (b) between model output and in situ observations after adding a third satellite product to each two-product assimilation combination, shown for selected vegetation types. Error bars denote 95% confidence intervals, and numbers below represent the sample size, which is identical across all groups. The label "all" denotes the simultaneous assimilation of L-band, C-band, and X-band data, while "double" refers to the assimilation of only two of them, which can be either L and C, L and X, or C and X.

21. Figure 10: A number of comments on this figure:

21.1 The whole discussion here seems to contradict the findings from Figure 9, where the conclusion was that adding X-band only had minimal impact on the skill or even degraded the performance.

Response:

Thanks for your suggestions. This misleading impression was caused by our improper arrangement of the paragraph structure in the original text. To eliminate the ambiguity caused by our writing, we have reordered the discussion of Figure 10 in the revised manuscript. We now discuss Figure 10a first, followed by Figures 10b and 10c. The revised content (Lines 615-640) is as follows:

Consistent with the spatially averaged results, for the station in NET Temperate area (Figure 14a). The time-series correlation for DA_ALL (0.53) was lower than that of DA_L+C (0.63). As can be seen, during June 2–20, the soil moisture from MWRI (brown squares) is notably higher than that of the other two products and in situ observations. This results in the soil moisture analysis from the DA_ALL experiment being significantly higher than that from DA_L+C, which clearly demonstrates that erroneous information in the MWRI product degrades the final assimilation performance.

In contrast, for the Corn vegetation type (Figure 14c), the DA_ALL experiment showed the highest accuracy, achieving a correlation of 0.83 with station data, compared to 0.56 for the CTL and 0.79 for the DA_L+C experiment. The inclusion of MWRI (X-band) data improved the model's ability to capture soil moisture responses to rainfall events, especially when SMAP (L-band) and ASCAT (C-band) data were unavailable on certain days (e.g., July 12). During the mid-July precipitation event, all experiments captured the sharp increase in soil moisture, but DA_ALL (the orange curve) reproduced both the peak (July 11) and the subsequent dry-down (July 12–13) with greater fidelity. At the non-Arctic grassland site (Figure 14b), the improvement derived from MWRI data is more prominent. The correlation in DA_ALL reached 0.43, compared to 0.23 for DA_L+C. MWRI demonstrates a strong capability in reproducing localized peaks in soil moisture, such as those on June 22 and June 27. It also well captures the three-wave variation characteristics of soil moisture during the period from June 27 to July 17, which constitutes a major reason for the significant increase in the correlation coefficient.

21.2 Could you please clarify how the three stations that are shown here are selected?

Could you include information on where they are located? And also, please comment on or show how the impact of adding X-band at these stations compares to other stations of the same land cover.

Response:

Thanks for your suggestions. Following your suggestions, we added the coordinates of the three representative stations in the main text and figure captions. We also clarified that these three stations were randomly selected from in situ sites with continuous observations for their corresponding vegetation types. Furthermore, the performance of these three random stations is consistent with the overall spatial average conclusions for their respective vegetation types presented in Figure 13. While Figure 13 shows that the addition of the X-band generally leads to performance degradation in densely vegetated areas (NET Temperate), this is precisely what is illustrated by the single station in Figure 14a. Meanwhile, the performance in sparsely vegetated areas such as croplands and grasslands shown in Figure 13 is reflected in Figures 14b and 14c through the mechanism of filling temporal gaps. Therefore, the time-series analysis of these stations provides specific mechanistic explanations and empirical cases for the regional statistical assessments in Figure 13. The revised content (Lines 611–613) is as follows:

To ensure objectivity and representativeness, three stations were randomly selected from different representative land cover types: NET Temperate (-83.39°, 33.78°), non-Arctic grassland (105.23°, 37.40°), and Corn (121.06°, 42.39°).

21.3 Please define the 'AWS' acronym for the in situ data in the caption or just label the green line 'in situ'.

Response:

Thanks for your suggestions. Following your suggestions, we have uniformly changed the label for the green solid line from 'AWS' to 'In-situ' in Figure 14 and other relevant figures. This modification not only more directly indicates the in-situ observation data but also avoids any confusion caused by unnecessary abbreviations.

21.4 The blue and black dots for the C- and X-band retrievals are difficult to tell apart. I suggest using different marker symbols to make it easier to distinguish them.

Response:

Thanks for your suggestions. Following your suggestions, we have applied different geometric shapes to represent the different satellite products. The L-band (SMAP) is now represented by red dots, the C-band (ASCAT) by blue diamonds, and the X-band (MWRI) by brown squares. The modified figure has been updated in the manuscript (and is presented here as Figure R9 for your convenience).

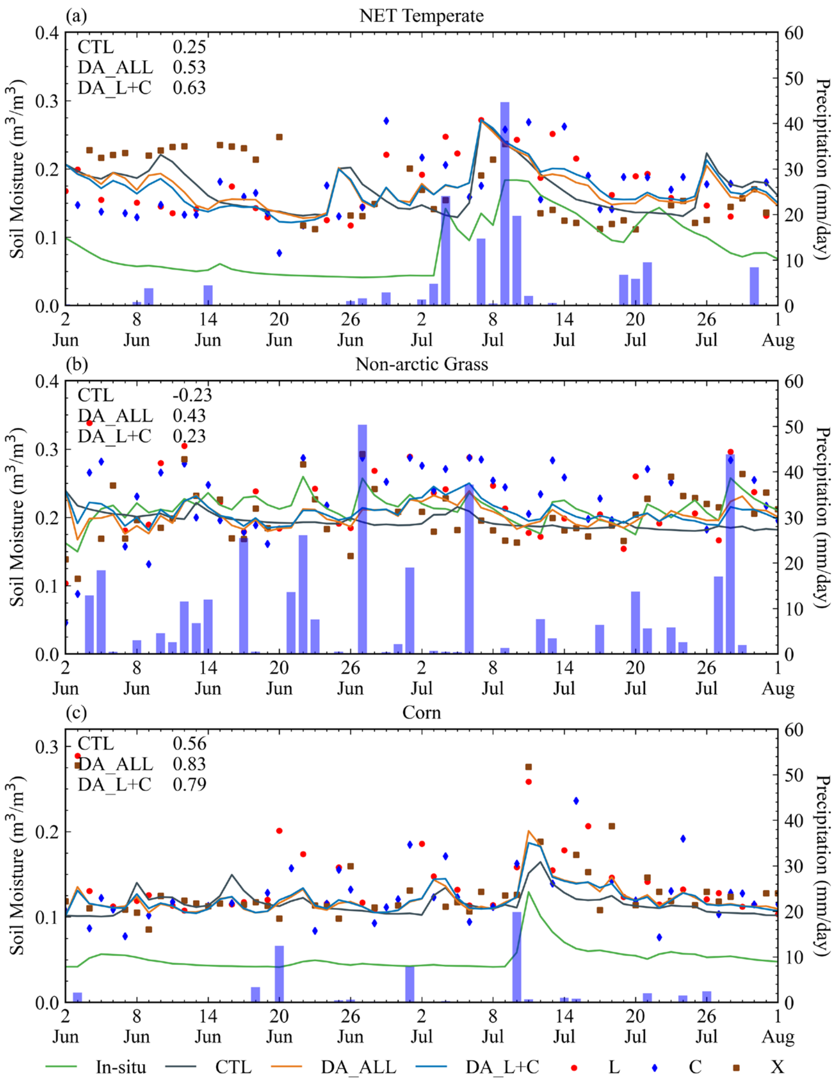

Figure R9: Time series of daily mean soil moisture from model simulations, satellite retrievals, and in situ observations for different assimilation experiments. The green solid line represents in situ observations. Black, orange, and blue solid lines indicate soil moisture simulations from the control experiment, the DA_ALL assimilation experiment, and the DA_L+C assimilation experiment, respectively. Red dots, blue diamonds, and brown squares represent L- (SMAP),

C- (ASCAT), and X-band (MWRI) satellite soil moisture products, respectively. Blue bars denote daily precipitation.

22. ll.367-369: Could you please include information on how the threshold for including X-band observations was defined?

Response:

Thanks for your suggestions. Regarding the threshold definition for introducing X-band observations, rather than using a quantitative threshold, we primarily established the assimilation selection threshold in this study based on the vegetation type classification of the CoLM. Specifically, land cover types including bare soil, arctic grass, non-arctic grass, grass, corn, and wheat were categorized as "sparsely vegetated regions." We have added these detailed definitions to the revised manuscript to ensure clarity (Lines 662–663).

23. Figure 12: I do not quite follow why a different reference was used for the central-west and south-east regions in the bottom plots. Could you please clarify?

Response:

Thanks for your suggestions. Our primary purpose was to visually demonstrate the contrasting relative impacts of the X-band in sparsely and densely vegetated areas, respectively. In the Midwest (sparsely vegetated areas), introducing the X-band is beneficial; therefore, we used DA_L+C as the baseline to show the positive improvement brought by its addition. Conversely, in the Southeast (densely vegetated areas), introducing the X-band leads to a degradation in assimilation performance; thus, we used DA_ALL as the baseline to more intuitively highlight this negative effect, because neither the NEW experiment nor the DA_L+C experiment assimilated MWRI data in this domain, so the advantages of the new scheme cannot be demonstrated from NEW-DA_L+C.

we have added a clear explanation in the revised manuscript (Lines 693–696). The revised content is as follows:

To comprehensively evaluate the specific contribution of the MWRI (X-band) product, this study employed a region-specific comparative strategy. In densely vegetated regions, where the assimilation weight of the X-band data is dynamically set to zero, the focus is on comparing the NEW experiment with the DA_ALL experiment. Conversely, in sparsely vegetated regions, the comparison primarily focuses on the differences between the NEW and DA_L+C experiments.

24. Figure 12 and 13 In the discussion of both figures the focus seems to be on the skill improvements of NEW compared to the CTL. I think it would also be relevant to discuss here how NEW compares to the L+C+X assimilation experiment that does not use the vegetation-adaptive approach.

Response:

Thanks for your suggestions. Following your suggestions, we have supplemented Figures 12 and 13 with this information in the revised manuscript.

The content added to Figure 12 (Lines 696–703) is as follows:

"Quantitative analysis reveals that in the sparsely vegetated central-western region of China, the inclusion of X-band data improved the correlation coefficient by 0.014. This improvement occurs because X-band microwave signals experience minimal canopy attenuation in low-biomass areas, allowing the retrievals to reliably capture surface soil moisture dynamics and provide valuable supplementary information. Meanwhile, in the densely vegetated region, the new assimilation scheme achieved a correlation improvement of 0.1 compared to the DA_ALL experiment. In such dense canopies, high-frequency X-band signals are strongly affected by vegetation, which increasing retrieval uncertainty. By dynamically masking these degraded observations, the adaptive scheme prevents the assimilation of erroneous data, thereby realizing this performance gain."

The content added to Figure 13 (Lines 715–717) is as follows:

"The spatial distribution of differences between the NEW experiment and the baselines (DA_L+C and DA_ALL) reveals negative values across most regions, indicating an overall ubRMSE reduction of approximately 0.001 m^3/m^3. Furthermore, compared to the improvements in correlation, the reduction in ubRMSE is relatively limited."